

Design and thermodynamic analysis of a pathway enabling anaerobic production of poly-3-hydroxybutyrate in *Escherichia coli*

Olavarria, Karel; Sousa, Diana Z.; van Loosdrecht, Mark C.M.; Wahl, S. Aljoscha

DOI

[10.1016/j.synbio.2023.09.005](https://doi.org/10.1016/j.synbio.2023.09.005)

Publication date

2023

Document Version

Final published version

Published in

Synthetic and Systems Biotechnology

Citation (APA)

Olavarria, K., Sousa, D. Z., van Loosdrecht, M. C. M., & Wahl, S. A. (2023). Design and thermodynamic analysis of a pathway enabling anaerobic production of poly-3-hydroxybutyrate in *Escherichia coli*. *Synthetic and Systems Biotechnology*, 8(4), 629-639. <https://doi.org/10.1016/j.synbio.2023.09.005>

Important note

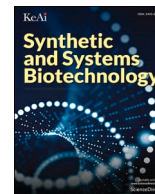
To cite this publication, please use the final published version (if applicable). Please check the document version above.

Copyright

Other than for strictly personal use, it is not permitted to download, forward or distribute the text or part of it, without the consent of the author(s) and/or copyright holder(s), unless the work is under an open content license such as Creative Commons.

Takedown policy

Please contact us and provide details if you believe this document breaches copyrights. We will remove access to the work immediately and investigate your claim.



Original Research Article

Design and thermodynamic analysis of a pathway enabling anaerobic production of poly-3-hydroxybutyrate in *Escherichia coli*

Karel Olavarria^{a,b,*}, Marco V. Becker^c, Diana Z. Sousa^{a,b}, Mark C.M. van Loosdrecht^c, S. Aljoscha Wahl^d

^a Laboratory of Microbiology, Wageningen University and Research, Stippenenweg 4, 6708 WE, Wageningen, The Netherlands

^b Centre for Living Technologies, Eindhoven-Wageningen-Utrecht Alliance, Princetonlaan 6, 3584 CB, Utrecht, The Netherlands

^c Department of Biotechnology, Applied Sciences Faculty, Delft University of Technology, van der Maasweg 9, 2629 HZ, Delft, The Netherlands

^d Lehrstuhl für Bioverfahrenstechnik, Friedrich-Alexander-Universität, Paul-Gordan-Strasse 3, 91052, Erlangen, Germany



ARTICLE INFO

Keywords:

Pathway feasibility analysis
Protein cost
Anaerobic metabolism
Engineered pathways
Metabolite concentrations

ABSTRACT

Utilizing anaerobic metabolisms for the production of biotechnologically relevant products presents potential advantages, such as increased yields and reduced energy dissipation. However, lower energy dissipation may indicate that certain reactions are operating closer to their thermodynamic equilibrium. While stoichiometric analyses and genetic modifications are frequently employed in metabolic engineering, the use of thermodynamic tools to evaluate the feasibility of planned interventions is less documented. In this study, we propose a novel metabolic engineering strategy to achieve an efficient anaerobic production of poly-(R)-3-hydroxybutyrate (PHB) in the model organism *Escherichia coli*. Our approach involves re-routing of two-thirds of the glycolytic flux through non-oxidative glycolysis and coupling PHB synthesis with NADH re-oxidation. We complemented our stoichiometric analysis with various thermodynamic approaches to assess the feasibility and the bottlenecks in the proposed engineered pathway. According to our calculations, the main thermodynamic bottleneck are the reactions catalyzed by the acetoacetyl-CoA β -ketothiolase (EC 2.3.1.9) and the acetoacetyl-CoA reductase (EC 1.1.1.36). Furthermore, we calculated thermodynamically consistent sets of kinetic parameters to determine the enzyme amounts required for sustaining the conversion fluxes. In the case of the engineered conversion route, the protein pool necessary to sustain the desired fluxes could account for 20% of the whole cell dry weight.

1. Introduction

Stoichiometric analyses have become invaluable tools for a deeper understanding of complex metabolic networks and the rational design of metabolic engineering strategies [1,2]. However, the metabolic network analyses restricted to the stoichiometric relationships are blind to important factors such as the thermodynamic feasibility of the involved reactions or the kinetic properties of the participating enzymes. Consideration of kinetic and thermodynamic constraints is frequently crucial for the success of metabolic engineering approaches [3–5]. Therefore, we think that the inclusion of thermodynamic and kinetic analyses is an important step during the assessment of the feasibility of the metabolic engineering strategies.

Two methods used for the identification of possible thermodynamic and kinetic bottlenecks in metabolic pathways are the Max-Min Driving

Force (MDF) [6] and the Enzyme Cost Minimization (ECM) [7,8]. MDF calculates the maximum possible thermodynamic driving force of the conversion pathway, given a set of metabolite concentration ranges [6]. It aids in identifying the reactions and metabolite concentrations that are key for the thermodynamic feasibility and favorability of the conversion. On the other hand, the ECM method calculates the minimum amount of enzyme required to sustain a given metabolic flux through a conversion pathway. Thus, the comparison between the experimentally observed amount of a given enzyme (which could be determined by enzymatic assays, proteomics, immunoassays, etcetera) and the minimal amount calculated by ECM could guide the genetic engineering approaches towards a cellular resource allocation more suitable for the biotechnological purpose.

MDF and ECM methods are particularly valuable for analyzing anaerobic conversions, which dissipate less free energy and thus have

Peer review under responsibility of KeAi Communications Co., Ltd.

* Corresponding author. Laboratory of Microbiology, Wageningen University and Research, Stippenenweg 4, 6708 WE, Wageningen, the Netherlands.

E-mail address: karel.olavarriagamez@wur.nl (K. Olavarria).

<https://doi.org/10.1016/j.synbio.2023.09.005>

Received 24 June 2023; Received in revised form 14 September 2023; Accepted 19 September 2023

Available online 27 September 2023

2405-805X/© 2023 The Authors. Publishing services by Elsevier B.V. on behalf of KeAi Communications Co. Ltd. This is an open access article under the CC BY-NC-ND license (<http://creativecommons.org/licenses/by-nc-nd/4.0/>).

narrower ranges of thermodynamically feasible intracellular metabolite concentrations. Despite the thermodynamic constraints, anaerobic conversions offer two key advantages compared to aerobic processes: (i) reduced material and/or energy input (no air supply, low stirring and less cooling) and (ii) increased product yields. Remarkably, previous thermodynamic analyses have shown that many biotechnologically relevant products could be produced using anaerobic processes [9]. The implementation of metabolic engineering designs that enable the substitution of conventional aerobic conversions with anaerobic conversions has the potential to enhance the competitiveness and reduce the environmental footprint of certain bioprocesses. One such bioprocess is the production of poly-(R)-3-hydroxybutyrate (PHB).

PHB is a polymer that can be synthesized by various microorganisms, and it has properties similar to some petrol-based plastics. In 1988, two research groups independently showed that the expression of the *pha-CAB1* gene from *Cupriavidus necator* is sufficient to induce PHB accumulation in *Escherichia coli* [10,11]. Since these groundbreaking studies, the study of PHB accumulation in *E. coli* has attracted considerable attention given the large availability of tools to genetically modify this bacterium and its natural inability to degrade this polymer. In addition, *E. coli* can assimilate different carbon sources and it can grow both aerobically and anaerobically.

Carlson and co-workers studied anaerobic PHB production in *E. coli*. They combined experimental observations with analysis of the stoichiometric possibilities, specifically focusing on elementary modes enabling the highest possible product yields, given the glycolytic pathways naturally present in this bacterium [12]. The study concluded that the co-supply of glucose and acetate, in a 2:1 ratio, should result in the production of (R)-3-hydroxybutyryl monomers and formic acid, in a 1:1 ratio, allowing for the recovery of 80% of the carbon in the PHB.

Experimentally, the anaerobic co-generation of PHB and ethanol [13–15] or PHB and hydrogen [16] have been achieved. However, the obtained PHB yield are very low (6 mg^{PHB}/g^{glucose} [16]; 8 mg^{PHB}/g^{xylose} [14]; 14 mg^{PHB}/g^{xylose} [15]). Moreover, the continuous generation of PHB as the sole fermentation product during anaerobic metabolism has not been reported yet. We are proposing here a novel metabolic engineering strategy for *E. coli* to achieve an anaerobic conversion of glucose or sucrose into PHB, while maximizing product yield and ATP output. In addition to the stoichiometric analysis, MDF and ECM calculations were applied to identify key bottlenecks in the proposed engineered route, assessing the thermodynamic and biological feasibility of this strategy. Moreover, we employed these computational tools to compare the proposed engineered conversion pathway with the natural glycolytic pathways from *E. coli*.

2. Methods

A visual representation of the workflow connecting the stoichiometric, thermodynamic and kinetic analyses is provided in Fig. S1.

2.1. Stoichiometric analyses

All the stoichiometric analyses were performed by Flux Balance Analyses, using the COBRA Toolbox (v3.0) for MATLAB [17]. The anaerobic conversion routes from glucose/sucrose to PHB analyzed in this study were outlined as lists of stoichiometrically balanced reactions (see Supplementary Material). These routes are (i) the Embden-Meyerhof-Parnas (EMP), (ii) the Entner-Doudoroff (ED) and (iii) the engineered conversion route proposed in this report (Tables S1–S4). When considering the putative substrate channeling between the acetoacetyl-CoA β -ketothiolase (EC 2.3.1.9) and the acetoacetyl-CoA reductase (EC 1.1.1.36), the following lumped reaction was employed: 2 Acetyl-CoA + NADH \rightleftharpoons Coenzyme A + (R)-3-hydroxybutyryl-CoA + NAD⁺.

For the calculations of the specific consumption/production (q-) rates and yields expected, without considering biomass formation, a

simple *in silico* glycolytic model was constructed, including the lists of stoichiometrically balanced reactions of the pathways under analysis. For the simulations of the growth-coupled PHB accumulation, an *in silico* model of *E. coli*, with experimentally validated values for the bioenergetics parameters (i) P/O ratio, (ii) growth dependent ATP cost and (iii) growth independent ATP for maintenance [18] was adapted to represent the proposed engineered conversion pathway.

The scripts employed for all the Flux Balance Analyses can be found at https://github.com/kolavarria/anaerobic_PHB (last access: 08/25/2023).

2.2. MDF and ECM calculations

For the MDF and ECM calculations, we employed the open-source eEquilibrator-API and the eEquilibrator-pathway tool included in the eEquilibrator suite [19,20], freely accessible at the website <http://equilibrator.weizmann.ac.il/> (last access: 06/19/2023). The complete python code (notebooks) can be accessed at: https://github.com/kolavarria/anaerobic_PHB (last access: 08/25/2023).

The MDF is an optimization problem that can be represented as:

$$\text{maximize } B$$

$$\text{subject to } -\Delta_r G' \geq B$$

$$\Delta_r G' = \Delta_r G^0 + RT \bullet S^T \bullet x$$

$$\ln(C_{min}) \leq x \leq \ln(C_{max})$$

where x is the metabolite log-concentrations vector, S^T is the transposed stoichiometric matrix of the involved reactions and B is the lower boundary for the driving forces of all reactions, *i.e.* the driving force in the bottleneck reaction(s). C_{min} and C_{max} are the minimum and maximum concentrations for each metabolite. The eEquilibrator suite utilizes the Component Contribution method [21] to estimate the standard Gibbs energies of formation of each compound, and from these energies of formation it calculates the standard Gibbs energy change ($\Delta_r G^0$) associated with each reaction. The values of temperature (310.15 K), ionic strength (200 mM) and cytoplasmic pH (7.5) used in Gibbs energy calculations correspond to the conditions typically employed to study *E. coli* in laboratory [6]. Metabolite concentration ranges were set following different criteria/sources. Whenever possible, experimentally determined values were assigned (Table S5).

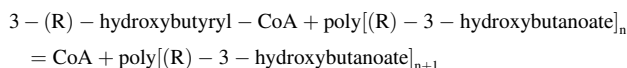
For the ECM calculations, the absolute fluxes through the enzyme-catalyzed reactions were calculated by Flux Balance Analysis, using the COBRA Toolbox for MATLAB. These absolute fluxes were calculated minimizing the glucose/sucrose uptake rate required to cover the ATP expenses for maintenance in *E. coli* ($m^{ATP} = 0.075 \text{ mol}^{ATP}/\text{Cmol}^{biomass}/\text{h}$ or $3.2 \text{ mmol}^{ATP}/\text{g}^{CDW}/\text{h}$ considering a biomass relative weight of 23.2 g^{CDW}/Cmol^{biomass} [18]). The quantitative relationship between the absolute fluxes and the amount of enzyme required to sustain the conversion fluxes is described in the Supplementary Material.

ECM calculations were performed with thermodynamically consistent sets of kinetic parameters obtained with the Parameter Balancing Tool. The Parameter Balancing Tool is a Bayesian estimation method which requires prior information about the probability distributions of the considered parameters. These distributions are represented by the mean values with their corresponding standard deviations. Although it is possible to run this method without previous available information about the kinetic parameters of the participating enzymes, the input of experimentally determined values increase the accuracy of the result. Ideally, for each parameter it should be provided an estimation of its mean value and its associated standard deviation. Missing values are replaced by values obtained from a population with a probability distribution characterized by a default mean and standard deviation. This

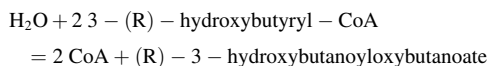
method assumes that the rates of the reactions under analysis can be described with modular rate laws [22]. The reversible Michaelis-Menten equation is one special case of the modular rate laws. Thus, whenever possible, we provided, as input for the Parameter Balancing Tool, estimates of the mean and the standard deviation of the turnover constants (in the forward and the backward directions) and the Michaelian constants. To execute the Parameter Balancing Tool, we accessed to the website https://rumo.biologie.hu-berlin.de/pb/static/css/css_template/main.html (last access: 06/19/2023). The input and output files can be accessed at: https://github.com/kolavarria/anaerobic_PHB (last access: 08/25/2023).

2.3. Treatment of the PHB polymerization reaction

The final step of PHB synthesis is the polymerization reaction:



where n represents the number of monomers of 3-(R)-hydroxybutyryl contained in the growing polymer of PHB. The polymerization to obtain PHB is a rather complex process, with the formation of a compound in solid state (zero activity). This reaction, catalyzed by the PHB synthase, is irreversible in the physiological conditions. Strictly, each step of elongation will have a (slightly) different standard Gibbs energy of formation. To simplify our analysis, a proxy reaction was used to represent the polymerization: the formation of (R)-3-hydroxybutanoyloxybutanoate (KEGG compound C04546) from two molecules of 3-(R)-hydroxybutyryl-CoA:



Mechanistically, each further elongation of the polymer goes through the same set of broken and formed bonds. We assumed that the use of this proxy reaction should not drastically affect the calculation of the MDF. However, the use of the same proxy reaction in the ECM analyses introduced an artificially higher cost due to its reversibility ($\Delta_r G^\circ = -13.9 \pm 10.0$ kJ/mol). Thus, the proxy reaction was not considered in the calculations of enzyme cost.

2.4. Concentration variability analysis

Analogously to Flux Variability Analysis [23], we developed a Concentration Variability Analysis (CVA). CVA calculates the concentration range for the metabolite i such that the resulting thermodynamic driving forces of the reactions considered in the network be equal to or higher than a defined value (B_{input}). Therefore, CVA can be formulated as the following optimization problem:

$$\begin{aligned} & \text{minimize } \ln(C_i), \text{ maximize } \ln(C_i) \\ & \text{subject to } -\Delta_r G' \geq B_{\text{input}} \\ & \Delta_r G' = \Delta_r G'^0 + RT \bullet S^T \bullet x \\ & \ln(C_{\text{min}}^*) \leq x^* \leq \ln(C_{\text{max}}^*) \end{aligned}$$

In the CVA, a specific metabolite log-concentration $\ln(C_i)$ is minimized and maximized in two different linear optimizations in order to obtain the minimum and maximum concentrations that allow an MDF value equal or higher than B_{input} . The log-concentrations vector x^* and the respective concentration bounds vectors C_{min}^* and C_{max}^* include all the metabolites considered in the network except the metabolite i , which is not constrained during the CVA optimization.

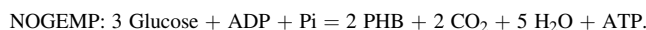
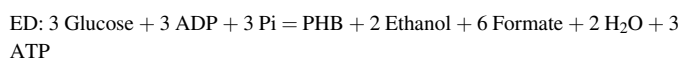
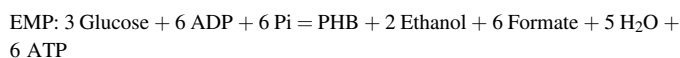
3. Results and discussion

3.1. A novel strategy towards an efficient anaerobic production of PHB

In wild type *E. coli* cells, glucose can be converted to acetyl-CoA with a positive ATP yield, through two glycolytic routes: the Embden-Meyerhof-Parnas (EMP) and the Entner-Doudoroff (ED) pathways, complemented with the reactions catalyzed by the pyruvate formate lyase (EC 2.3.1.54) (Fig. 1A). A stoichiometric analysis of these catabolic routes shows a mismatch between the amount of acetyl-CoA and reducing equivalents produced by these pathways and the amount of acetyl-CoA and reducing equivalents required by the PHB biosynthetic route (Fig. 1B). Consequently, to achieve the redox balance for PHB production from sugars under anaerobic conditions, it is necessary that cells co-produce another fermentation product [14], take-up volatile fatty acids [24], or use an external electron acceptor [25]. In this study, we are proposing an alternative solution to overcome this mismatch by generating a fraction of the acetyl-CoA through the non-oxidative glycolysis. The non-oxidative glycolysis (NOG) is an artificial pathway, firstly proposed by Bogorad and co-workers, enabling the conversion of glucose into acetate without oxidation steps [26]. Specifically, if 75% of the acetyl-CoA is generated by-passing the oxidation steps catalyzed by the glyceraldehyde-3-phosphate dehydrogenase and the pyruvate dehydrogenase complex, the resulting proportion of acetyl-CoA and reducing equivalents matches the redox requirements for PHB synthesis (Fig. 1C). Therefore, it should be feasible to design a metabolic engineering strategy that combines reactions from the NOG and EMP pathways. Thus, we will refer to this new strategy as NOGEMP.

The implementation of NOGEMP can be divided in five modules. *First*, glucose uptake must occur by diffusion [27], and glucose-6-phosphate must be produced in a reaction catalyzed by a glucokinase (EC 2.7.1.2) to uncouple the phosphorylation of glucose from the flux through the lower EMP or ED pathways. *Second*, the upper glycolytic flux should go through the NOG. For this redirection of the glycolytic flux, phosphoketolase (EC 4.1.2.9) and fructose-1,6-biphosphatase (EC 3.1.3.11) activities are required [26]. The 6-phosphofructokinase (EC 2.7.1.11) activity must be suppressed to avoid an ATP futile cycle caused by the simultaneous activities of phosphofructokinase and fructose-1,6-biphosphatase [28]. *Third*, the reduction of acetoacetyl-CoA to 3-(R)-hydroxybutyryl-CoA must be catalyzed by an NADH-preferring acetoacetyl-CoA reductase (EC 1.1.1.36) [25]. This will transform PHB in a sink for the electrons carried by NADH (*i.e.*, a fermentation product). *Fourth*, the formation of ethanol, acetate and lactate must be suppressed [29]. The suppression of the mentioned products enforces PHB synthesis as an obligate mechanism for NADH re-oxidation and avoids the conversion of acetyl-CoA to acetate. The formation of succinate and formate/H₂ cannot be fully suppressed because it is required for biomass formation under anaerobic conditions. *Fifth*, modifications in the promoter region controlling the expression of the genes encoding for the pyruvate dehydrogenase complex are required to become active under anaerobic conditions [30]. Overall, the implementation of the five previously described modules will imply that, under anaerobic conditions, PHB accumulation will be coupled to biomass formation.

If we consider the dimer of two monomers of (R)-3-hydroxybutyrate as the minimal unit of PHB, the global reactions of the anaerobic conversion of glucose to PHB using the EMP, the ED or the NOGEMP are:



The comparison of the yields of these conversion pathways

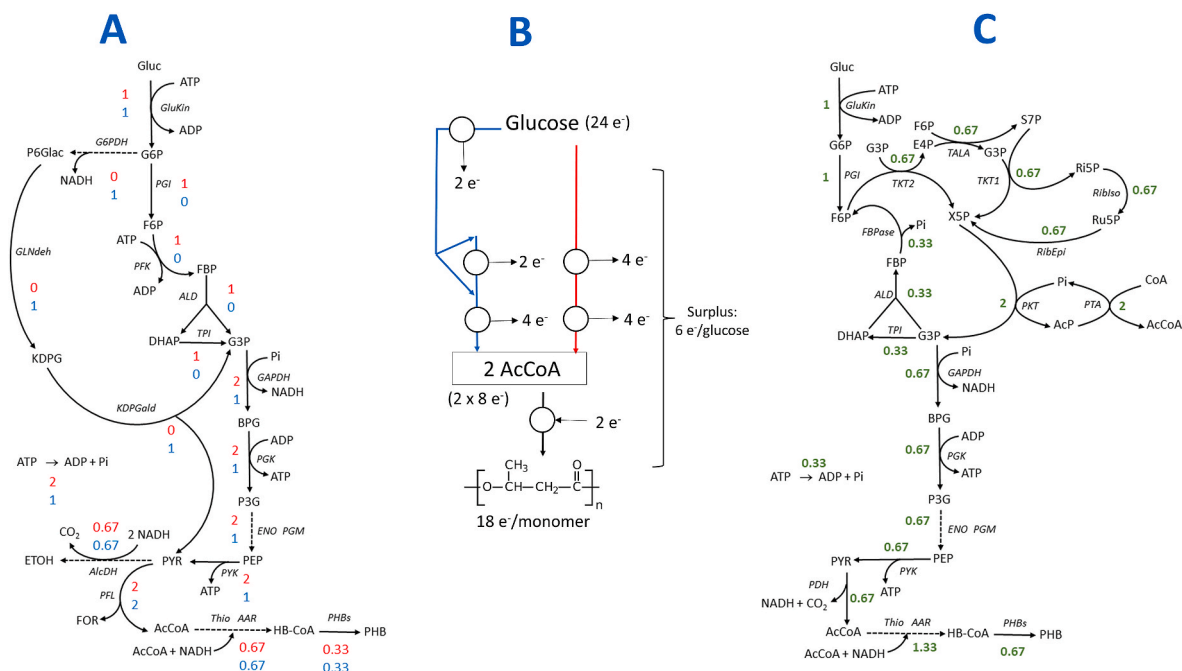


Fig. 1. Efficient PHB accumulation requires a match between acetyl-CoA (AcCoA) and electrons. **A:** In *E. coli* wild type, glucose is oxidized through the Embden-Meyerhof-Parnas (EMP) and/or the Entner-Doudoroff (ED) pathways. The numbers represent the relative metabolic fluxes through the EMP (red) and the ED (blue) pathways, respect to one molecule of oxidized glucose. The harvested ATP is “consumed” in an ATP hydrolysis reaction, mimicking the ATP consumed for maintenance or other metabolic processes. Names of the metabolites and enzymes are detailed in the Supplementary Material. **B:** It is possible to see that, either using the EMP (red arrow) or the ED pathway (blue arrows), there is a mismatch between the catabolic supply of AcCoA and reducing equivalents and the demand of AcCoA and reducing equivalents of the PHB synthesis pathway: for every two molecules of AcCoA generated, four pairs of electrons must be harvested by NAD, NADP or released as formate/H₂. However, only one NAD(P)H is re-oxidized during the synthesis of 3-(R)-hydroxybutyrate (the monomer of the PHB). The other molecules of NAD(P)H have to be re-oxidized in processes delivering electrons outside of the cells (respiration or fermentation). Circles represent enzymatic steps catalyzed by oxido-reductases. **C:** Proposed engineered pathway enabling an efficient anaerobic conversion of glucose to PHB. Due to the combination of reactions from the Embden-Meyerhof-Parnas and the Non-Oxidative Glycolysis pathways, we nicknamed this engineered pathway as NOGEMP. Note that all the reducing equivalents coming from the carbon source can be harvested in the product, approaching the maximum theoretical product yield. Names of the metabolites and enzymes are detailed in the Supplementary Material.

highlights the advantage of implementing the NOGEMP pathway: 90% of the carbon and 100% the electrons contained in the source should be conserved in the product (Table 1). The improvements in the production yields are due to the correction of the mismatch between the acetyl-CoA and the electrons produced in the oxidation of the glucose and the acetyl-CoA and electrons consumed in the PHB formation, eliminating the necessity of generating fermentation products.

However, our stoichiometric analyses do not consider the thermodynamic characteristics of the intermediary reactions and the kinetic properties of the involved enzymes. To overcome these limitations, we firstly focused on the identification of the thermodynamic bottlenecks in NOGEMP and the assessment of the metabolite concentration ranges enabling the operation of this pathway.

3.2. Max-Min Driving Force analyses show that the reaction catalyzed by the acetoacetyl-CoA β -ketothiolase is the main thermodynamic bottleneck

The thermodynamic driving forces of the ED, EMP and NOGEMP

Table 1

Specific consumption/production (q-) rates and yields expected for the operation of the pathways under analysis.

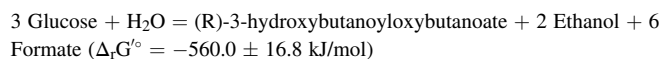
Pathway	q _{glucose}	q _{Ethanol}	q _{Formate}	q _{ATP}	q _{PHB}	y _{carbon*} (Cmol in PHB/Cmol in glucose)	Y ^{**} (g ^{PHB} /g _{glucose})	fraction of y ^{max#} (%)
EMP	-15	10	30	30	5	0.444	0.32	50
ED	-15	10	30	15	5	0.444	0.32	50
NOGEMP	-15	0	0	5	10	0.889	0.64	100

* The PHB molecule was considered as the union of two monomers of 3-R-hydroxybutyrate.

** The molecular weight of the considered PHB molecule is 172 g/mol.

Maximum theoretical yield.

pathways were compared using a wide concentration range (between 1 μ M and 10 mM). The ED pathway exhibited the highest thermodynamic driving force, while the NOGEMP pathway had the lowest thermodynamic driving force (MDF_{EMP} = 8.53 kJ/mol, MDF_{ED} = 11.38 kJ/mol, MDF_{NOGEMP} = 7.17 kJ/mol). Previous studies have shown that, in the absence of PHB synthesis reactions, the MDF of ED is higher than that of EMP [7]. According to Flamholz and co-workers, the higher ATP conservation for EMP comes with a price: a lower MDF and a higher enzyme cost. Our results show that, even with the inclusion of PHB synthesis reactions and considering a wide metabolite concentration range, ED still has a higher MDF than EMP. It must be noticed that the products generated in the EMP and ED in one hand, and NOGEMP in the other hand, are not the same. According to the calculations with the group contribution method [21], the free energy variation of the global reactions of these pathways differs:



3 Glucose = 2 (R)-3-hydroxybutanoyloxybutanoate + 2 CO₂ + 4 H₂O ($\Delta_r G^\circ = -639.4 \pm 15.6$ kJ/mol)

This difference impacts the potential for energy conservation. However, the stoichiometric analysis shows that despite its higher total free energy variation, NOGEMP showed the lowest ATP conservation and the lowest MDF value. This indicates the co-existence in the same pathway of steps with a large energy dissipation (the reactions catalyzed by phosphoketolase and fructose-1,6-biphosphatase) and steps with a low metabolic driving force (the linked and highly reversible reactions catalyzed by phosphoglucose isomerase (EC 5.3.1.9), transaldolase (EC 2.2.1.2), transketolase (EC 2.2.1.1), ribose-5-phosphate isomerase (EC 5.3.1.6) and ribose-5-phosphate epimerase (EC 5.1.3.1)) (Fig. S2).

MDF calculations were repeated, this time considering experimentally validated narrower ranges of metabolite concentrations to estimate the thermodynamic driving forces at physiological conditions (Table S5). The results (MDF_{EMP} = 6.17 kJ/mol, MDF_{ED} = 6.62 kJ/mol, MDF_{NOGEMP} = 3.77 kJ/mol) show that the thermodynamic driving forces of all three pathways decreased due to the more constrained metabolite concentration ranges (Fig. S2). However, it is important to note that all three pathways remained feasible under these physiological conditions.

To gain a deeper understanding of the factors limiting the achievable thermodynamic force in the pathways under analysis, a concentration variability analysis (CVA) was implemented. This analysis aimed to determine the metabolite concentration ranges that enable the operation of a given pathway at a specific thermodynamic driving force. At the thermodynamic driving force calculated by the MDF analysis, at least one of the metabolites reached a critical concentration threshold. This means that the concentration of that particular metabolite fell outside the range that enables thermodynamic feasibility of at least one reaction. Therefore, CVA calculations must be performed by setting the thermodynamic driving force at a value lower or equal to the thermodynamic driving force calculated by MDF. As expected, the higher the allowed thermodynamic driving force, the more constrained were the metabolite concentration ranges that enable the achievement of such thermodynamic driving force (Fig. 2, Fig. S3). CVA also enabled us to calculate which are the metabolites with extreme concentrations during

the operation of the pathway, even at a low thermodynamic driving force. For this purpose, we performed CVA analyses setting the thermodynamic driving force at 1 kJ/mol. In the three analyzed pathways, minimal acetyl-CoA concentrations of 4.8 mM and maximal acetoacetyl-CoA concentrations of 21 μ M are required to enable the operation of any of the three pathways under analysis, at a thermodynamic driving force of 1 kJ/mol (Table S9). These metabolites with extreme concentrations indicate that the reaction catalyzed by the acetoacetyl-CoA β -ketothiolase is the primary thermodynamic bottleneck, as it involves both acetyl-CoA and acetoacetyl-CoA.

The reaction catalyzed by the acetoacetyl-CoA β -ketothiolase is a Claisen condensation between two molecules of acetyl-CoA with a standard free energy of +25.2 kJ/mol. Substrate channeling has been observed in other enzymes catalyzing reactions with a similar functional chemistry, such as the 3-ketoacyl-CoA thiolase participating in the β -oxidation in *Pseudomonas fragi* [31], the citrate synthase in the Krebs cycle in pigs [32] and the acetoacetyl-CoA reductase participating in the formation of 3-hydroxy-3-methylglutaryl-CoA in the mevalonate pathway from Archaea [33]. Therefore, it is likely that substrate channeling plays a role during the formation of PHB, as previously suggested [25,34]. The finding of experimental evidence of this phenomenon requires dedicated biochemical procedures beyond the scope of this research. Yet, we explored the effects of substrate channeling between the acetoacetyl-CoA β -ketothiolase and the acetoacetyl-CoA reductase on the thermodynamic profile of the anaerobic conversion of glucose in PHB, using the EMP, ED and NOGEMP pathways. For the analyses of the effect of substrate channeling, the reactions catalyzed by the acetoacetyl-CoA β -ketothiolase and the acetoacetyl-CoA reductase were replaced by the lumped reaction $2 \text{ AcCoA} + \text{NADH} \rightarrow (\text{R})\text{-3-hydroxybutyryl-CoA} + \text{CoA} + \text{NAD}^+$. Consistent with the hypothesis of considering the reaction catalyzed by the acetoacetyl-CoA β -ketothiolase as the thermodynamic bottleneck in the three pathways, higher driving forces were obtained using the lumped reaction (MDF_{EMP} = 7.05 kJ/mol, MDF_{ED} = 8.16 kJ/mol, MDF_{NOGEMP} = 4.67 kJ/mol). Moreover, the concentration variability analyses showed a decrease in the minimal concentration of acetyl-CoA required to have feasible conversions

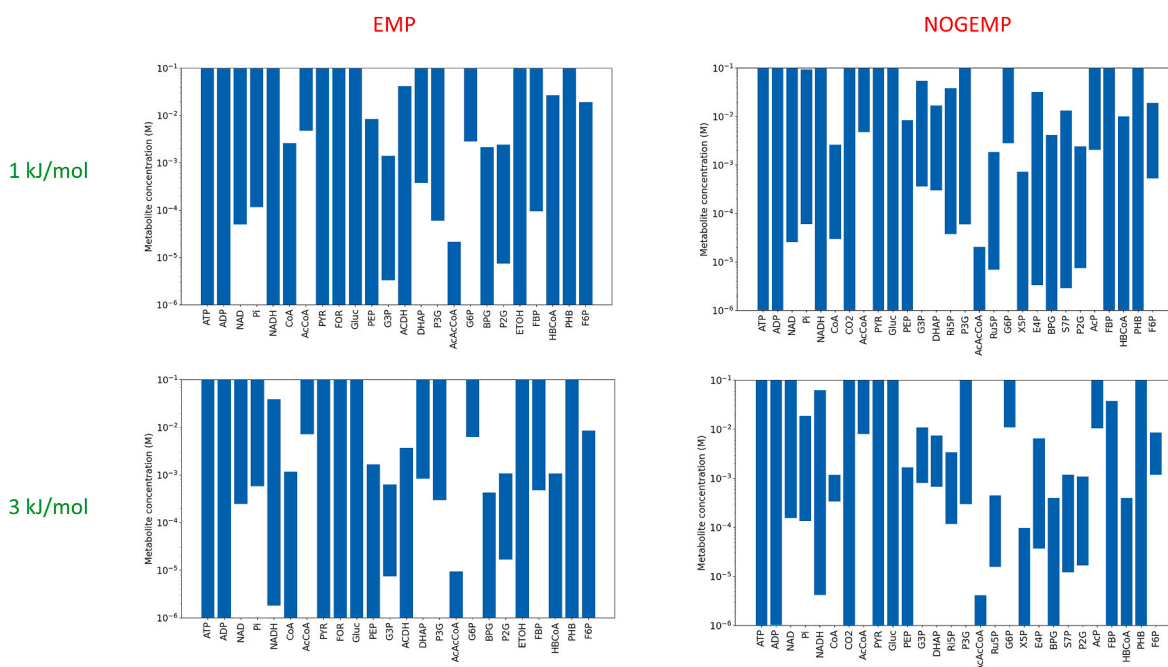


Fig. 2. Metabolite concentration ranges enabling the operation of the EMP and NOGEMP pathways at two different driving forces (1 kJ/mol and 3 kJ/mol). The limits of the ordinate axes were fixed at convenient values, not necessarily corresponding to the thermodynamically feasible metabolite concentrations ranges. These metabolite concentration ranges were obtained with the Concentration Variability Analysis approach. It is possible to see how some metabolite concentration ranges are constrained with the increase in the thermodynamic driving force; for example, the range for the acetoacetyl-CoA (AcAcCoA).

(Tables S10–S12). Bearing in mind a cytoplasmic volume of 1.9 mL/gCDW [35] and the molecular weight of the acetyl-CoA (809.57 g/mol), the change in the minimal concentration of acetyl-CoA from 4.8 mM to 0.12 mM due to the substrate channeling, implies a decrease from 0.7% to 0.02% in the contribution of acetyl-CoA to the cellular weight. Given the large molecular weight of the coenzyme A and the thermodynamic constraints associated with the Claisen condensation, it seems likely that some mechanism enabling a substrate channeling between the acetoacetyl-CoA β -ketothiolase and the acetoacetyl-CoA reductase had been developed by evolution. However, given the lack of experimental evidence and to avoid bias, the rest of the calculations here reported were performed without considering this substrate channeling mechanism.

Our MDF calculations show that the reaction catalyzed by the acetoacetyl-CoA β -ketothiolase is the main thermodynamic bottleneck for the anaerobic production of PHB using the EMP, the ED or the engineered NOGEMP pathway. Previous experimental observations of PHB accumulation in *E. coli* cells under anaerobic conditions showed that this thermodynamic bottleneck can be surpassed [12,36]. However, to achieve the flux distribution envisioned in the proposal of the NOGEMP, an extensive re-wiring of the metabolic fluxes is required. Provided that (i) the enzymes catalyzing the formation of fermentation products are eliminated by genetic engineering and that (ii) the enzymes participating in NOGEMP are expressed in the required amounts, the only way to re-oxidize the produced NADH under anaerobic conditions is with the flux distribution proposed for NOGEMP. The elimination of the enzymes involved in the generation of fermentation products can be achieved by genetic engineering, using techniques described elsewhere [25,37]. On the other hand, to calculate the *minimal amount of the enzymes* required to sustain the metabolic fluxes, we applied the ECM approach.

3.3. NOGEMP pathway could be sustained by *E. coli* cells after further modifications aiming an increase in ATP conservation

For the ECM calculations, we defined the absolute fluxes as the metabolic fluxes required to sustain the ATP cost for maintenance (see Supplementary Material for a more detailed explanation). The respective ATP yields (Table 2) and fluxes distributions (Fig. S4) were calculated by Flux Balance Analysis. Kinetic parameters found in literature come from diverse experiments, executed under different conditions; therefore, taken as a whole they could be inconsistent with the laws of thermodynamics. To obtain more accurate results, the turnover rates (in the forward and the backward direction) and the Michaelis constants of a given enzyme should be thermodynamically consistent, satisfying the corresponding Haldane relationship. To accomplish this requirement, thermodynamically consistent sets of kinetic parameters were obtained using the Parameter Balancing Tool [38] (Fig. S1, Table S8). To run the Parameter Balancing Tool, we constructed (i) SBML models representing each pathway and (ii) the corresponding *.tsv files containing the estimated means and standard deviations of the equilibrium constants and the kinetic parameters. The files containing the SBML models were constructed using the freely available tool COPASI (v4.34) [39]. For the construction of the *.tsv files, experimentally determined parameters

were gathered from different sources (see values and references in Table S6). The uncertainties associated to the equilibrium constants were taken directly from the estimations of eQuilibrator. The uncertainties associated to the known kinetic parameters were taken from the literature (when available) or declared as unknown values (when information about the dispersion of the kinetic estimates was not available in the reviewed literature). Overall, for all the pathways under study, more than 70% of the parameters employed as input for the Parameter Balancing Tool were known (Table S7). Certainly, the number of unknown values affects the accuracy of the obtained results: the larger the number of unknown values, the larger the uncertainties associated with the calculated consistent parameters. The resulting sets of thermodynamically consistent kinetic parameters, with their associated uncertainties, are available in Table S8.

After including the molecular weight of the participating enzymes, the ECM analysis yielded their results in units of grams of protein per liter of cytoplasm ($\text{g}^{\text{Prot}}/\text{L}^{\text{Cyt}}$). This conversion enabled to evaluate the physiological impact of the protein cost, calculated as the fraction of the total cellular protein pool occupied by the enzymes of a given pathway. To calculate these fractions, we considered that every liter of cytoplasm corresponds to 526 g of cell dry weight [35], and that proteins account for 70% of the cell dry weight [18]. The resulting equation is:

$$\frac{\text{enzyme cost} \left(\frac{\text{g}^{\text{Prot}}}{\text{L}^{\text{Cyt}}} \right)}{526 \frac{\text{g}^{\text{CDW}}}{\text{L}^{\text{Cyt}}} * 0.7 \frac{\text{g}^{\text{Prot}}}{\text{g}^{\text{CDW}}}} * 100\%$$

The protein fractions obtained for the different pathways are shown in Table 2. Our results show that the combined contributions of the glycolytic enzymes, without considering acetoacetyl-CoA β -ketothiolase and acetoacetyl-CoA reductase, is 6.21 $\text{g}^{\text{Prot}}/\text{L}^{\text{Cyt}}$ for the ED pathway and 8.55 $\text{g}^{\text{Prot}}/\text{L}^{\text{Cyt}}$ for the EMP pathway. This indicates that, despite its higher ATP yield, the amount of protein required for the operation of the EMP pathway is higher than the amount required for the ED pathway, which is consistent with previous observations [7]. Considering the costs of acetoacetyl-CoA β -ketothiolase plus acetoacetyl-CoA reductase in the EMP and the ED pathways, these enzymes contribute with 3.33 $\text{g}^{\text{Prot}}/\text{L}^{\text{Cyt}}$ and 4.68 $\text{g}^{\text{Prot}}/\text{L}^{\text{Cyt}}$, respectively. Due to the fact that the ATP yield of the ED pathway is half of the ATP yield of the EMP pathway, to cover the same ATP cost for maintenance the flux through the enzymes acetoacetyl-CoA β -ketothiolase and acetoacetyl-CoA reductase in the ED pathway doubles the flux through the same enzymes in the EMP pathway (Fig. S4). Nevertheless, the protein cost of these enzymes in the ED pathway does not double the cost of these enzymes in the EMP pathway because the thermodynamic conditions are different for each pathway (Tables S10 and S11). This case exemplifies how the contribution to the whole proteome of a subset of enzymes, with identical kinetic properties, could be different, depending on the thermodynamic conditions found in each network. This calculation is an example of a (biotechnologically) relevant information that it is possible to get with the thermodynamic and kinetic analyses and that it is not possible to get with simple stoichiometric analyses.

In the case of the NOGEMP pathway, the enzyme cost raises to 126 $\text{g}^{\text{Prot}}/\text{L}^{\text{Cyt}}$. One of the reasons explaining this higher cost is the higher glycolytic flux required to cover the same ATP expenses for maintenance

Table 2
Physiological impact of the enzyme cost.

	ATP yield ($\text{mol}^{\text{ATP}}/\text{mol}^{\text{hexose}}$)	enzyme cost ($\text{g}^{\text{Prot}}/\text{L}^{\text{Cyt}}$)	contribution Thio + AAR to whole enzyme cost (% of enzyme cost)	contribution of the pathway to whole proteome (%)
ED	1	10.9	43	3.0
EMP	2	11.9	28	3.2
NOGEMP	0.333	126.4	25	34.3
NOGEMP sucrose symporter	0.667	72.4	23	20
NOGEMP sucrose uniporter	1.667	60.5	22	16

but using a glycolytic network with a lower ATP yield (Table 1). On the other hand, as previously addressed, the NOGEMP has more reactions operating closer to their thermodynamic equilibrium; therefore, at a given time, more active sites are engaged in catalyzing backward reactions, increasing the amount of enzyme required to sustain a given net flux in the forward direction [8].

The enzyme cost calculated for NOGEMP would represent 34% of the whole cellular proteome. This number exceeds the estimated fractions of the whole proteome dedicated to the catabolic functions (between 10% [40,41] and 20% [42]). To overcome this problem, we are proposing to increase the ATP conservation by fueling the cells with sucrose instead of glucose, followed by sucrose phosphorolysis [43]. Two mechanisms were considered for the transport of sucrose across the cytoplasmic membrane: (i) facilitated diffusion through a uniporter and (ii) co-transport of sucrose with protons (Fig. S5). In the latter case, one molecule of sucrose is co-transported with one proton. To maintain the cytoplasmic pH, the excess of protons is pumped out the cytoplasm. The amount of ATP required to pump-out one mol of protons depends on the difference in pH between the cytoplasm and the periplasmic compartment, the transmembrane voltage and the concentrations of ATP, ADP and Pi. According to our calculations, three mol of proton can be pumped-out with the energy released by the hydrolysis of one mol of ATP (see calculations in the Supplementary material and Table S13). Therefore, depending on the sucrose uptake mechanism, the ATP yield should rise to 0.667 ATP/hexose (sucrose symporter) or to 1.667 ATP/hexose (uniporter).

After implementing the strategies to increase the ATP conservation, the enzyme cost of NOGEMP should decrease, representing 20% (symporter) or 16% (uniporter) of the whole proteome (Table 2). Although these values are in the upper half of the previously reported range of 10–20% of the proteome dedicated to catabolism, it is important to highlight that these previously reported values are based on aerobic growth. It has been shown that during the shift from aerobic to anaerobic conditions most of the newly formed proteins are involved in glycolysis and pathways aimed at preventing glycolysis grinding to a halt by a cellular redox imbalance [44]. Moreover, it has been observed that, during anaerobic conditions, the abundance of the proteins

associated with glycolysis and fermentation is duplicated and the abundance of the enzymes of the Krebs cycle are reduced up to five times [45]. In this scenario, alcohol dehydrogenase, pyruvate formate lyase, enolase and glyceraldehyde-3-phosphate dehydrogenase represented each one 2–3% of the proteome mass.

Regarding the choices to increase the ATP conservation, it is key to discuss that although the passive diffusion of sucrose had been described in different plants [46–48] and some data support its successful heterologous expression in *Saccharomyces cerevisiae* [43], other data indicate that the actual operative mechanism is a proton:sucrose symporter [49]. Even if sucrose diffusion is possible, the feasibility of this mechanism will depend on the existence of a concentration gradient between the extracellular medium and the cytoplasm. Considering that the Michaelis constants for sucrose of the best studied sucrose phosphorylases are around 10–20 mM [50], the semi-saturation of this enzyme would require intracellular concentrations of sucrose above 3.5 g/L. Therefore, even considering its higher cost in comparison with the sucrose uniporter, we consider that the implementation of the strategy based on the use of a proton:sucrose symporter is more safe. Complementary approaches such as directed evolution and protein/genomic engineering could help to decrease the enzyme cost.

We would also want to highlight that the ECM analysis yielded insights into the contributions of the thermodynamic, saturation, and capacity terms to the costs of individual enzymes (Fig. 3, Fig. S6). This information is valuable because it allows to assess the potential for reducing enzyme costs through improvements in the catalytic efficiency of the involved enzymes. While protein engineering approaches cannot change the thermodynamic properties of a given reaction, the availability of faster and/or more saturated enzyme can lead to a decrease in enzyme costs.

3.4. Oxygen-limited cultures could increase PHB yield

In the previous section, we estimated the fractions of the proteome dedicated to sustain the glycolytic flux required to cover the ATP costs for maintenance. However, the actual glycolytic flux (and its associated enzyme cost) will be higher after considering the resources required to

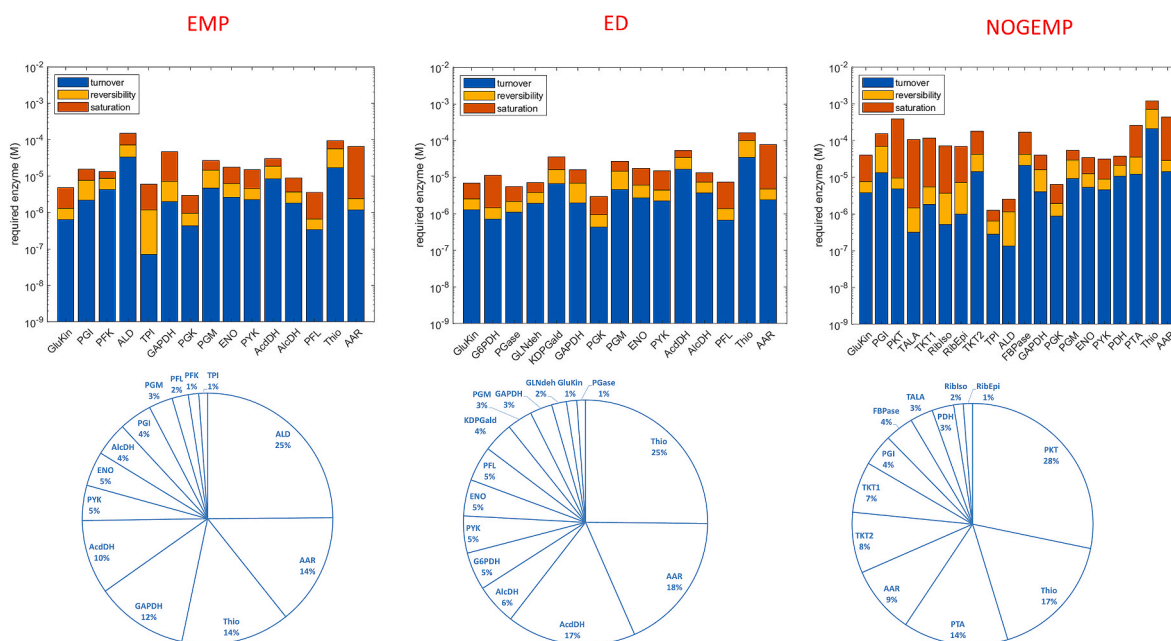


Fig. 3. Relative contributions of the thermodynamic driving force (reversibility), catalytic power of the enzyme (turnover) and metabolite concentrations (saturation) to the enzyme costs, according to the results of the ECM analysis, for the EMP, ED and NOGEMP pathways (stacked bars graphics). In the Supplementary Material it is shown how these contributions were calculated. Using the molecular weights of the polypeptides, the corresponding masses were calculated and plotted (pie charts). Proteins whose contributions were below 1% were not represented in the pie charts.

make biomass. One possibility to decrease the glycolytic flux required to cover the ATP demands is to “burn” a fraction of the taken-up carbon source by oxidative phosphorylation, a process that yields a much larger amount of ATP per hexose. With the aim to quantify the effect on the PHB accumulation of implementing a limited supply of oxygen, we expanded the stoichiometric analysis including the reactions required for the tricarboxylic acid cycle, oxidative phosphorylation and biomass synthesis. Sucrose uptake was implemented as a proton:sucrose symporter. Two different cultivation modes were simulated: (i) a sucrose-limited continuous culture with different levels of oxygen supply, and (ii) a batch culture with different levels of oxygen supply. For the simulation of the continuous culture, the growth rate was fixed to 0.05 h^{-1} (corresponding to the biomass composition of the employed *in silico* model [18]) and the optimization goal was the minimization of the sucrose consumption rate. On the other hand, for the simulation of the batch culture, sucrose uptake rate was fixed to 10 mmol/gCDW/h (according to experimentally observed sucrose uptake rates in *E. coli* W [51]) and maximization of the biomass formation was set as the optimization goal. To evaluate the effect of the maintenance ATP costs, the simulations were executed for two experimentally obtained values of this bioenergetics parameter: $3.2 \text{ mmol}^{\text{ATP}}/\text{gCDW/h}$ [18] and $16.4 \text{ mmol}^{\text{ATP}}/\text{gCDW/h}$ [52].

According to our simulations, both for the case of a continuous culture or a culture in batch, the increase in the oxygen supply, until a certain critical value, increases the PHB yield (Fig. 4 and Fig. S7). However, an increase in the oxygen supply beyond this critical value decreases the PHB yield. The oxygen consumption rates corresponding to the critical value change depending on the culture setup and the maintenance ATP cost. The reason behind this behavior is that the availability of oxygen enables the re-oxidation to menaquinone of the menaquinol generated in the anabolic reaction catalyzed by the dihydroorotate dehydrogenase (EC 1.3.5.2) without requiring the formation of succinate in the reaction catalyzed by the succinate dehydrogenase (EC 1.3.5.1). Therefore, with the increase in the availability of oxygen until the critical value, a lower flux through the succinate dehydrogenase is required for the re-oxidation of the menaquinol generated in the anabolism. This relationship between the oxygen availability, the

production of succinate and the PHB yield can be appreciated both in the continuous culture and the culture in batch (Fig. 4 and Fig. S7). Beyond the critical value (zero succinate production), the supply of oxygen exceed the amount required for the re-oxidation of menaquinol and it drains electrons that otherwise can be sink in the PHB. Using the previously described approach, the PHB content could reach values of 80–90% of the total cell weight, which is comparable with the highest values reported for *E. coli* [53,54], but with a yield of $0.74 \text{ g}^{\text{PHB}}/\text{g}^{\text{hexose}}$ (batch) or $0.92 \text{ g}^{\text{PHB}}/\text{g}^{\text{hexose}}$ (continuous) which would be two times higher than the values of $0.36\text{--}0.4 \text{ g}^{\text{PHB}}/\text{g}^{\text{hexose}}$ previously reported [53, 54].

Using a limited supply of oxygen, the amount of proteins required to sustain glycolysis will decrease but other proteins will be required. However, many of the enzymes required for the oxidation of glucose/sucrose have to be expressed anyways to generate the building blocks of the biomass. Nevertheless, the use of oxygen implies more operational costs. Still, another possibility to implement the proposed metabolic engineering approach is to divide the whole biotechnological process into a phase of aerobic biomass formation followed by a phase of anaerobic PHB accumulation. Anyways, the actual costs will depend on many factors, and a techno-economical evaluation of what is the more profitable option is beyond the scope of this manuscript.

3.5. On the experimental implementation of NOGEMP in *E. coli*

According to our stoichiometric analysis, the NOGEMP pathway enables the coupling of PHB accumulation and NADH re-oxidation, with net ATP generation. In the Supplementary Material we outlined a possible genetic engineering strategy to materialize this metabolic engineering proposal. Currently, there is a handful of techniques to efficiently perform gene knock-in/out and modulate the gene expression. A specific discussion about which is the most suitable genetic tool to implement the NOGEMP is beyond the scope of this paper. However, we acknowledge the necessity of elaborate more about some key parts or modules required for the functioning of the engineered pathway.

First, it should be noticed that the pyruvate dehydrogenase activity is required to implement the NOGEMP. The most effective way to achieve

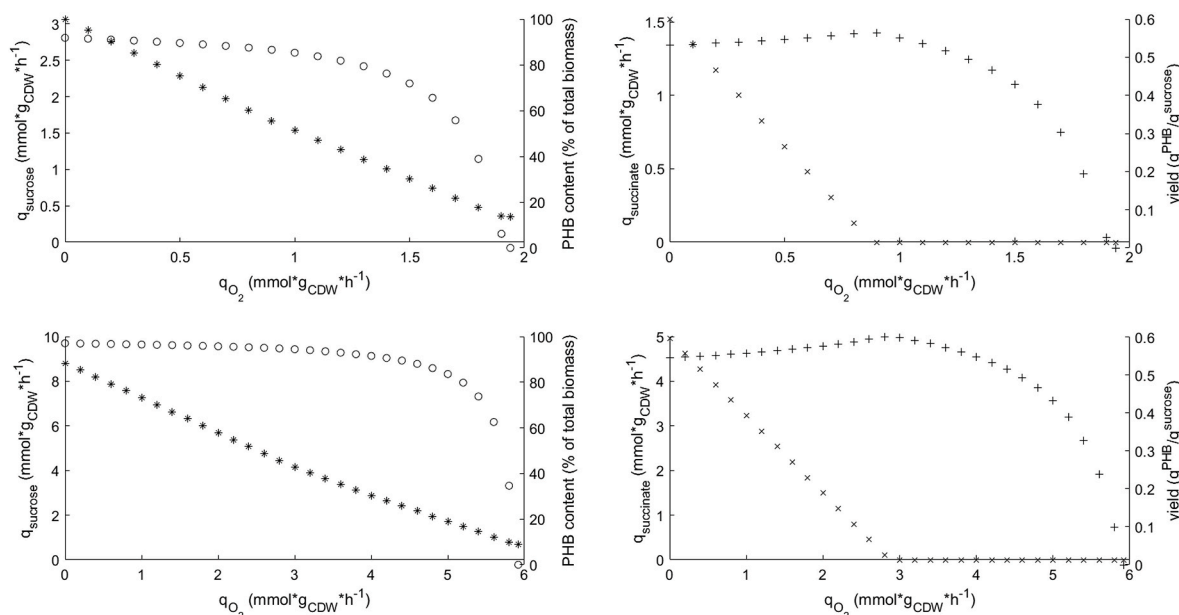


Fig. 4. Different production parameters as a function of the oxygen consumption rate (q_{O_2}) for a continuous culture ($D = 0.05 \text{ h}^{-1}$) of engineered *E. coli* cells with the NOGEMP pathway, using sucrose as the sole carbon source. Different production parameters as a function of the oxygen consumption rate (q_{O_2}). Two different maintenance ATP costs were considered during the calculations: $3.2 \text{ mmol}^{\text{ATP}}/\text{gCDW/h}$ (upper row) and $16.4 \text{ mmol}^{\text{ATP}}/\text{gCDW/h}$ (lower row). Shown values correspond to the simulation of a continuous culture with a dilution rate of 0.05 h^{-1} . On the left side, sucrose consumption rate (*) and PHB content (o); on the right side, succinate production rate (x) and PHB yield (+).

pyruvate dehydrogenase activity under anaerobic conditions in *E. coli* is through the modification of the regulatory elements in the promoter, as already published [55–57]. Another alternative would be to maintain the usual anaerobic conversion of pyruvate to AcCoA catalyzed by the pyruvate formate lyase (E.C. 2.3.1.54), but substituting the formate dehydrogenase (E.C. 1.17.1.9) from *E. coli* (which use menaquinone as cofactor) by the NAD-dependent formate dehydrogenase from *Candida boidinii* [58].

Second, our choice for the acetoacetyl-CoA reductase was the engineered enzyme obtained by a combination of structural elements from the protein encoded by the *phaB1* from *C. necator* and an acetoacetyl-CoA dehydrogenase isolated from *Candidatus Accumulibacter phosphatis* [59]. The resultant enzyme (Chimera 5) has a high preference for NADH under physiological conditions and one of the highest turnover recorded among the kinetically characterized homologues.

Third, the functionality of the NOGEMP depends on the operation of the synthetic non-oxidative glycolysis [26]. The key step in this pathway is the reaction catalyzed by a phosphoketolase. The phosphoketolase from *Bifidobacterium adolescentis* seems a good choice, as it has both xylulose-5-phosphate-dependent (E.C. 4.1.2.9) and fructose-6-phosphate-dependent (E.C. 4.1.2.22) activities, and it is functional in *E. coli* [26,28]. Moreover, it was already successfully expressed in a previous effort aiming an increase in PHB production [60].

The introduction of the non-oxidative glycolysis implies that two thirds of the glycolytic flux goes to acetyl-CoA, skipping oxidation steps, and that a smaller flux goes through the lower EMP. This modification decreases the NADH yield per hexose and matches the catabolic production and the PHB-linked consumption of NADH. Remarkably, this smaller flux through the lower EMP rules out the use of the PEP phosphotransferase system to fuel the glucose uptake because the flux through the reaction catalyzed by a PEP synthase (E.C. 2.7.9.2) required to replenish the PEP pool would imply zero net ATP production. On the other hand, the decreased flux through the lower EMP implies a decrease in the ATP yield per hexose, increasing the absolute flux required to cover the ATP expenses, stretching the enzyme cost. To overcome this situation, we propose (i) to extend the metabolic engineering intervention to include the passive diffusion and phosphorolysis of sucrose and/or (ii) the use of oxygen-limiting cultures.

An important observation arising from our calculations is the potential role of substrate channeling in PHB accumulation. The molecular mechanisms of substrate channeling and the positive effect of multi-enzyme assemblies and scaffolds for reaction kinetics are current subjects of debate [61,62]. Engineering spatial proximity between multiple enzymes of a metabolic cascade has been shown to increase product titers in other cases [63]. Indeed, the three enzymes enabling the formation of PHB from acetyl-CoA have been physically approximated in *E. coli* with the use of molecular scaffolds, and an increase of 2.5-fold in PHB production was observed after the introduction of such modification [34].

To represent the substrate channeling in our calculations, we used the approach proposed by Bar-Even and co-workers, where the reactions involved in a substrate channeling event can be considered as a single lumped reaction [6,64]. Although it has not been extensively elaborated, that model assumes the transfer of intermediates between two enzymes as a change between different transition states of the net reaction. The existence of this kind of transition states is not considered in the typical calculations of Δ_rG' . This model remains to be experimentally validated, but if it is indeed validated, MDF, CVA and ECM analyses would be powerful tools for identifying reactions likely engaged in substrate channeling. In any case, for the final calculations of the enzyme costs, substrate channeling was not considered.

There are two important potential limitations of our approach that require some discussion. First, for the estimations of the enzyme costs, we based our calculations in the fluxes required to cover $3.2 \text{ mmol}^{\text{ATP}}/\text{g}_{\text{CDW}}/\text{h}$ for maintenance. Values as high as $16.4 \text{ mmol}^{\text{ATP}}/\text{g}_{\text{CDW}}/\text{h}$ had

been previously reported for *E. coli* growing under anaerobic conditions [52]. However, this latter value was obtained assuming a different value of P/O ratio and in the presence of acetate, which could cross back into the cytoplasm as acetic acid and dissociate inside the cells. The dissociation of the acetic acid generates protons, and the pumping-out of these protons cost energy. In our proposed approach, the generation of acetate should be decreased or suppressed by genetic engineering. The second important limitation is that the protein costs determined by ECM correspond to the most favorable thermodynamic driving force (MDF) calculated for a simplified network. It is possible that the actual metabolite concentrations ranges are more constrained because other reactions (anabolism) need to be thermodynamically feasible as well. The smaller the MDF, the higher the protein cost because the enzymes will be operating in a less favorable thermodynamic situation. Nevertheless, it is possible that some of the design choices defined in our strategy may themselves enhance the thermodynamic driving forces. Non-oxidative glycolysis has been shown to significantly increase acetyl-phosphate concentrations (likely increasing acetyl-CoA concentrations as well) [26]. Additionally, the deletion of genes involved in the formation of ethanol and lactate could increase the NADH/NAD ratio as it eliminates potential electron sinks other than PHB. Moreover, the suppression of the formation of acetate should eliminate a process draining acetyl-CoA.

Finally, it is important to address that, as steady state based optimization algorithms, both MDF and ECM may not accurately predict *in vivo* dynamic conditions, but these methods can be effective tools for identifying key factors hindering the effectiveness of a metabolic engineering strategy [65]. They are, definitively, a very useful complement to stoichiometry-based tools such as Flux Balance Analysis or the Elementary Modes Analysis, as they consider thermodynamic and kinetic properties of the reactions conforming the conversion network.

4. Conclusions

In this study, different approaches were combined to evaluate the thermodynamic and physiological feasibility of an efficient anaerobic conversion of glucose/sucrose in PHB. It was shown how a handful of reactions and metabolites involved in a novel conversion strategy can have a drastic effect in its feasibility, highlighting key targets for eventual genetic modifications. Special interest deserve the reactions catalyzed by the acetoacetyl-CoA β -ketothiolase and the acetoacetyl-CoA reductase, where the presence of a substrate channeling mechanism and/or the availability/discovery/engineering of enzymes with higher turnover numbers could be game changers.

Declaration of competing interest

The authors declare that they have no known competing financial interests or personal relationships which have or could be perceived to have influenced the work reported in this article.

CRediT authorship contribution statement

Karel Olavarria: Conceptualization, Formal analysis, Writing – original draft, Writing – review & editing. **Marco V. Becker:** Formal analysis, Investigation, Methodology, Writing – original draft. **Diana Z. Sousa:** Funding acquisition, Writing – review & editing. **Mark C.M. van Loosdrecht:** Supervision, Writing – review & editing. **S. Aljoscha Wahl:** Conceptualization, Funding acquisition, Supervision, Writing – review & editing.

Acknowledgements

This work was supported by the joint research program NWO–FAPESP of the Dutch Organization for Scientific Research (NWO) and the Sao Paulo Research Foundation (FAPESP) (code NWO:

BBE.2017.013; code FAPESP: 2017/50249-6). The contributions of Karel Olavarria and Diana Z. Sousa were also supported by a SIAM Gravitation Grant (024.002.002) from the Dutch Ministry of Education, Culture and Science (OCW) and by the Centre for Living Technologies, a part of the Alliance TU/e, WUR, UU, UMC Utrecht (www.ewuu.nl). The contribution of Mark C.M. van Loosdrecht was supported by the SIAM Gravitation Grant (024.002.002).

Appendix A. Supplementary data

Supplementary data to this article can be found online at <https://doi.org/10.1016/j.synbio.2023.09.005>.

References

- Tomar N, De RK. Comparing methods for metabolic network analysis and an application to metabolic engineering. *Gene* 2013;521:1–14.
- Jing LS, et al. Database and tools for metabolic network analysis. *Biotechnol Bioproc Eng* 2014;19:568–85.
- van Maris AJ, et al. Homofermentative lactate production cannot sustain anaerobic growth of engineered *Saccharomyces cerevisiae*: possible consequence of energy-dependent lactate export. *Appl Environ Microbiol* 2004;70(5):2898–905.
- Bond-Watts BB, Bellerose RJ, Chang MC. Enzyme mechanism as a kinetic control element for designing synthetic biofuel pathways. *Nat Chem Biol* 2011;7(4):222–7.
- Nguyen N-P-T, et al. Revising the Weizmann process for commercial n-butanol production. *Nat Commun* 2018;9(1):3682.
- Noor E, et al. Pathway thermodynamics highlights kinetic obstacles in central metabolism. *PLoS Comput Biol* 2014;10(2):e1003483.
- Flamholz A, et al. Glycolytic strategy as a tradeoff between energy yield and protein cost. *Proc Natl Acad Sci U S A* 2013;110(24):10039–44.
- Noor E, et al. The protein cost of metabolic fluxes: prediction from enzymatic rate laws and cost minimization. *PLoS Comput Biol* 2016;12(11):e1005167.
- Cueto-Rojas HF, et al. Thermodynamics-based design of microbial cell factories for anaerobic product formation. *Trends Biotechnol* 2015;33(9):534–46.
- Slater SC, Voige WH, Dennis DE. Cloning and expression in *Escherichia coli* of the *Alcaligenes eutrophus* H16 poly-beta-hydroxybutyrate biosynthetic pathway. *J Bacteriol* 1988;170(10):4431–6.
- Schubert P, Steinbuechel A, Schlegel HG. Cloning of the *Alcaligenes eutrophus* genes for synthesis of poly-beta-hydroxybutyric acid (PHB) and synthesis of PHB in *Escherichia coli*. *J Bacteriol* 1988;170(12):5837–47.
- Carlson R, Wlaschin A, Srieñ F. Kinetic studies and biochemical pathway analysis of anaerobic poly-(R)-3-hydroxybutyric acid synthesis in *Escherichia coli*. *Appl Environ Microbiol* 2005;71(2):713–20.
- Carlson R, Srieñ F. Effects of recombinant precursor pathway variations on poly [(R)-3-hydroxybutyrate] synthesis in *Saccharomyces cerevisiae*. *J Biotechnol* 2006;124(3):561–73.
- de Las Heras AM, et al. Anaerobic poly-3-D-hydroxybutyrate production from xylose in recombinant *Saccharomyces cerevisiae* using a NADH-dependent acetoacetyl-CoA reductase. *Microb Cell Factories* 2016;15(1):197.
- Portugal-Nunes DJ, et al. Effect of nitrogen availability on the poly-3-D-hydroxybutyrate accumulation by engineered *Saccharomyces cerevisiae*. *Amb Express* 2017;7(1):35.
- Wang RY, et al. Enhanced co-production of hydrogen and poly-(R)-3-hydroxybutyrate by recombinant PHB producing *E. coli* over-expressing hydrogenase 3 and acetyl-CoA synthetase. *Metab Eng* 2012;14:496–503.
- Heirendt L, et al. Creation and analysis of biochemical constraint-based models using the COBRA Toolbox v.3.0. *Nat Protoc* 2019;14(3):639–702.
- Taymaz-Nikerel H, et al. Genome-derived minimal metabolic models for *Escherichia coli* MG1655 with estimated in vivo respiratory ATP stoichiometry. *Biotechnol Bioeng* 2010;107(2):369–81.
- Flamholz A, et al. eQuilibrator - the biochemical thermodynamics calculator. *Nucleic Acids Res* 2012;40:D770–5. Database issue.
- Beber ME, et al. eQuilibrator 3.0: a database solution for thermodynamic constant estimation. *Nucleic Acids Res* 2021;50(D1):D603–9.
- Mavrouniotis ML, et al. A group contribution method for the estimation of equilibrium constants for biochemical reactions. *Biotechnol Tech* 1988;2(1):23–8.
- Liebermeister W, Uhlenendorf J, Klipp E. Modular rate laws for enzymatic reactions: thermodynamics, elasticities and implementation. *Bioinformatics* 2010;26(12):1528–34.
- Gudmundsson S, Thiele I. Computationally efficient flux variability analysis. *BMC Bioinformatics* 2010;11:2–4.
- Guedes da Silva L, et al. Revealing the metabolic flexibility of "Candidatus accumilibacter phosphatis" through redox cofactor analysis and metabolic network modeling. *Appl Environ Microbiol* 2020;86(24).
- Olavarria K, et al. An NADH preferring acetoacetyl-CoA reductase is engaged in poly-3-hydroxybutyrate accumulation in *Escherichia coli*. *J Biotechnol* 2021;325:207–16.
- Bogorad IW, Lin T-s, Liao JC. Synthetic non-oxidative glycolysis enables complete carbon conservation. *Nature* 2013;502(7473):693–7.
- Weisser P, et al. Functional expression of the glucose transporter of *Zymomonas mobilis* leads to restoration of glucose and fructose uptake in *Escherichia coli* mutants and provides evidence for its facilitator action. *J Bacteriol* 1995;177(11):3351–4.
- Lin PP, et al. Construction and evolution of an *Escherichia coli* strain relying on nonoxidative glycolysis for sugar catabolism. *Proc Natl Acad Sci USA* 2018;115(14):3538.
- Tseng H-C, et al. Metabolic engineering of *Escherichia coli* for enhanced production of (R)- and (S)-3-Hydroxybutyrate. *Appl Environ Microbiol* 2009;75(10):3137–45.
- Haydon DJ, Quail MA, Guest JR. A mutation causing constitutive synthesis of the pyruvate dehydrogenase complex in *Escherichia coli* is located within the pdhR gene. *FEBS Lett* 1993;336(1):43–7.
- Ishikawa M, et al. Structural basis for channelling mechanism of a fatty acid beta-oxidation multienzyme complex. *EMBO J* 2004;23(14):2745–54.
- Bulutoglu B, et al. Direct evidence for metabolon formation and substrate channeling in recombinant TCA cycle enzymes. *ACS Chem Biol* 2016;11(10):2847–53.
- Vögeli B, et al. Archaeal acetoacetyl-CoA thiolase/HMG-CoA synthase complex channels the intermediate via a fused CoA-binding site. *Proc Natl Acad Sci U S A* 2018;115(13):3380–5.
- Tippmann S, et al. Affibody scaffolds improve sesquiterpene production in *Saccharomyces cerevisiae*. *ACS Synth Biol* 2017;6(1):19–28.
- Wang L, et al. An accurate method for estimation of the intracellular aqueous volume of *Escherichia coli* cells. *J Microbiol Methods* 2013;93:73–6.
- Wu F, et al. Biosynthesis of poly-(3-hydroxybutyrate) under the control of an anaerobically induced promoter by recombinant *Escherichia coli* from sucrose. *Molecules* 2022;27(1).
- Olavarria K, et al. Metabolism of sucrose in a non-fermentative *Escherichia coli* under oxygen limitation. *Appl Microbiol Biotechnol*. 2019;103:6245–56.
- Lubitz T, et al. Parameter balancing in kinetic models of cell metabolism. *J Phys Chem B* 2010;114(49):16298–303.
- Hoops S, et al. COPASI—a Complex Pathway Simulator. *Bioinformatics* 2006;22(24):3067–74.
- Li GW, et al. Quantifying absolute protein synthesis rates reveals principles underlying allocation of cellular resources. *Cell* 2014;157(3):624–35.
- Peebo K, et al. Proteome reallocation in *Escherichia coli* with increasing specific growth rate. *Mol Biosyst* 2015;11(4):1184–93.
- Yang L, et al. Principles of proteome allocation are revealed using proteomic data and genome-scale models. *Sci Rep* 2016;6:36734.
- Marques WL, et al. Combined engineering of disaccharide transport and phosphorylation for enhanced ATP yield from sucrose fermentation in *Saccharomyces cerevisiae*. *Metab Eng* 2018;45:121–33.
- Kramer G, et al. Proteome-wide alterations in *Escherichia coli* translation rates upon anaerobiosis. *Mol Cell Proteomics* 2010;9(11):2508–16.
- Mori M, et al. From coarse to fine: the absolute *Escherichia coli* proteome under diverse growth conditions. *Mol Syst Biol* 2021;17(5):e9536.
- Zhou Y, et al. A suite of sucrose transporters expressed in coats of developing legume seeds includes novel pH-independent facilitators. *Plant J* 2007;49(4):750–64.
- Chen L-Q, et al. Sugar transporters for intercellular exchange and nutrition of pathogens. *Nature* 2010;468:527.
- Chen L-Q, et al. Sucrose efflux mediated by SWEET proteins as a key step for phloem transport. *Science* 2012;335(6065):207–11.
- Marques WL, et al. Laboratory evolution and physiological analysis of *Saccharomyces cerevisiae* strains dependent on sucrose uptake via the *Phaseolus vulgaris* Suf1 transporter. *Yeast* 2018;35(12):639–52.
- Aerts D, et al. Consensus engineering of sucrose phosphorylase: the outcome reflects the sequence input. *Biotechnol Bioeng* 2013;110(10):2563–72.
- Mohamed ET, et al. Generation of an *E. coli* platform strain for improved sucrose utilization using adaptive laboratory evolution. *Microb Cell Factories* 2019;18(1):116.
- Chen X, et al. Synergy between C-13-metabolic flux analysis and flux balance analysis for understanding metabolic adaptation to anaerobiosis in *E. coli*. *Metab Eng* 2011;13(1):38–48.
- Lee SY, et al. Comparison of recombinant *Escherichia coli* strains for synthesis and accumulation of poly-(3-hydroxybutyric acid) and morphological changes. *Biotechnol Bioeng* 1994;44(11):1337–47.
- Li Y, et al. Enhancing the glucose flux of an engineered EP-bifido pathway for high poly(hydroxybutyrate) yield production. *Front Bioeng Biotechnol* 2020;8:517336.
- Zhou S, Iverson AG, Grayburn WS. Doubling the catabolic reducing power (NADH) output of *Escherichia coli* fermentation for production of reduced products. *Biotechnol Prog* 2010;26:45–51.
- Crowhurst N. Exploiting the anaerobic expression of pyruvate dehydrogenase for the production of biofuels. Department of Biology. London: Imperial College London; 2012.
- Maeda S, et al. Pyruvate dehydrogenase complex regulator (PdhR) gene deletion boosts glucose metabolism in *Escherichia coli* under oxygen-limited culture conditions. *J Biosci Bioeng* 2017;123:437–43.
- Shen CR, et al. Driving forces enable high-titer anaerobic 1-butanol synthesis in *Escherichia coli*. *Appl Environ Microbiol* 2011;77(9):2905.
- Olavarria K, et al. Engineering an acetoacetyl-CoA reductase from *Cupriavidus necator* toward NADH preference under physiological conditions. *Sci Rep* 2022;12(1):3757.
- Wang Q, et al. Engineering an in vivo EP-bifido pathway in *Escherichia coli* for high-yield acetyl-CoA generation with low CO₂ emission. *Metab Eng* 2019;51:79–87.

- [61] Ellis GA, et al. Artificial multienzyme scaffolds: pursuing in vitro substrate channeling with an overview of current progress. *ACS Catal* 2019;9:10812–69.
- [62] Sweetlove LJ, Fernie AR. The role of dynamic enzyme assemblies and substrate channelling in metabolic regulation. *Nat Commun* 2018;9. <https://doi.org/10.1038/s41467-018-04543-8>.
- [63] Zhang YHP. Substrate channeling and enzyme complexes for biotechnological applications. *Biotechnol Adv* 2011;29:715–25.
- [64] Bar-Even A. Does acetogenesis really require especially low reduction potential? *Biochim Biophys Acta* 2013;1827(3):395–400.
- [65] Hädicke O, et al. OptMDFpathway: identification of metabolic pathways with maximal thermodynamic driving force and its application for analyzing the endogenous CO₂ fixation potential of *Escherichia coli*. *PLoS Comput Biol* 2018;14(9):e1006492.